



In-silico approach to identify antiviral potent inhibitors against nsp4 of SARS-COV-2

Aamir Saeed¹, Huma Naseem^{* 2}, Nighat Shafi³, Hammad Ahmed², Tayyaba Faraz², Rasheeda Fatima² and Adnan Khan⁴

¹Department of Bioinformatics, Hazara university Mansehra, Mansehra-21120, **Pakistan**

²Department of Pharmaceutical Chemistry, Faculty of Pharmacy, Ziauddin University, Karachi-75600, **Pakistan**

³Department of Chemistry, Faculty of Science, University of Karachi, Karachi-75270, **Pakistan**

⁴Department of Biotechnology, International Islamic University, Islamabad-44000, **Pakistan**.

*Correspondence: huma.naseem@hotmail.com Received 19-05-2022, Revised: 28-06-2022, Accepted: 04-07-2022 e-Published: 09-07-2022

In the absence of effective therapy till now millions of people are dying due to severe acute respiratory syndrome corona virus 2 (SARS-CoV-2). To combat with this highly pathogenic virus, potent and less toxic therapeutic drugs are needed. Non-structural protein (NSP4) responsible for cytoplasmic rearrangements necessary for optimal SARS-CoV-2 replication has been identified as one of the potential drug targets in the development of antiviral agents. To identify promising therapeutic compounds against the imminent danger of COVID-19, present study was designed to predict a 3D-model of NSP4 protein and recognize selective inhibitors, followed by molecular docking with reported antiviral photochemical compounds. Homology modeling was done by using deposited sequence of NSP4 in NCBI database. SWISS MODEL was used to identify best PDB template 3vcb with a sequence similarity of 61.36 percent. To validate 200 reported antiviral photochemical compounds were docked against developed 3D-NSP4 model by using MoE software. Lowest binding energy candidates were chosen and screened for pharmacokinetics using the ADMETS server. NSP4 3D homology model showed potential binding interactions with all reported drugs. However, seven inhibitors were discovered with strongest binding energies ranging from -9.4838 to -15.7308 Kcal/Mol. In conclusion, this study presents a 3D model of NSP4 and helps understanding the molecular interactions at atomic level. Hence, this model could be suggested as an antiviral target for the development of novel anti-viral agents against COVID-19.

Keywords: NSP4, SARS-COV-2, Molecular docking, Homology Modeling, Covid-19

INTRODUCTION

Over the years the world is surrounded by infectious viral diseases. These diseases are caused by various types of viruses which include Middle East respiratory syndrome corona virus (MERS-CoV), avian influenza A/H₇N₉ and H₅N₁ viruses, Nipah virus and severe acute respiratory syndrome coronavirus (SARS-CoV). In *Homo sapiens*, virus is etiological factor responsible for this global pandemic COVID-19 (Astuti 2020; Zhu et al. 2019). In China Wuhan novel virus was primarily detected during December 2019 by using next generation sequencing which termed as severe acute respiratory syndrome corona virus 2 (SARS-CoV-2). World health organization (WHO) reported on March 11, 2020 in patients of respiratory tract infection with pneumonia and also recognized virus as outbreak in the worldwide (Guo et al. 2020; Li et al. 2020). Corona virus belongs to the class of enveloped viruses, comprises of non-segmented positive sense, single stranded RNA virus. It consists of sarbecovirus, orthodox corona Viviane subfamily that widely spread mammals and *homo sapiens* species

(Huang et al. 2020; Gupta 2019).

Till now, no drug has been approved or reported as a regimen in the treatment of patients infected with SARS-Co-2. Only symptomatic treatment has been given to the most critically ill patients. Globally, scientists through their extensive research efforts have been constantly working in order to find new viral drug targets to treat Covid-19 patients. Pharmaceutical industries are also playing a key role in the processing and protocols of drug designing and development in order to explore novel drug moieties (Balunas et al. 2005).

Computational techniques and modern medicinal chemistry methods are the most advanced tools used in the process of drug discovery. These methods not only reduced time, cost but also many hindrances in the drug development process. Molecular modeling, molecular dynamics, virtual screening, structure based and ligand based drug-designing are used as a powerful software based techniques to explore the pharmacodynamic-pharmacokinetic features of ligands and structure activity relationship between drug and targets (Meng et al. 2011;

López et al. 2011).

Despite of the various structure determination methods of biological macromolecules like NMR spectroscopy, X-Ray crystallography and cryo-electron microscopy, development of 3D structure of the target protein is still time taken and difficult to obtain. Homology Modeling is one of the efficient tools to generate structural model of the host proteins as well as identifying active and binding sites on protein. The homology models have been successfully used in ligand and structure based virtual screening approaches. In molecular modeling, docking is one of the most common structure based virtual screening approach, aims to find the best orientation adopted by a molecule within a binding pocket of a macromolecular target to give binding score for each docked pose [9]. In addition to this, a variety of docking algorithms have been used which helps in identifying the area of docked compounds that promote binding affinity of lig and-receptor complex as well as pharmacokinetic properties (ADMET: absorption, distribution, metabolism, excretion and toxicity) (Lipinski and Lombardo 2012).

Two-third genome of all types corona virus have codes for replicas polypeptide, such as pp1ab, having two overlapping open reading frames (ORFs), ORF1a and ORF1band treat viral protease to divide into 16 distinct types of non-structural protein (NSPs) that participating in transcription and replications (Boopathi et al. 2020; Cotten et al. 2013; Gupta et al. 2020).

There are several proteins that having non-structural domain in among of all sixteen proteins, for instances NSP3, NSP4 and NSP6. NSP3 connected to NSP4 in host cell, performed rearrangement of membrane in SARS-CoV-2 and this interaction is essential for viral replication (Sakai et al. 2017). The activity of NSP3, NSP4, and NSP6 was noticed in rotator cuff (RTC) disease and located within ER cells that expressed independently (Kanjanaaluethai et al. 2007; Oostra et al. 2007; Oostra et al. 2007). The one-third C-terminus of NSP3 interact with NSP4 was identified by immune precipitation technique.

The present study aims for identification and designing of potential therapeutic drugs against SARS-COV-2 NSP4 protein having vital role in replication of viral genome in host cells. We also addressed interaction of already reported inhibitors with corona virus in order to understand lig and-protein interaction.

MATERIALS AND METHODS

Data analysis of NSP4 protein sequence

The Fasta sequence of NSP4 protein having (Accession number YP_009742611.1) in SARS-COV-2 was obtained from NCBI database (<https://www.ncbi.nlm.nih.gov/>), While ProtParam tool (<http://web.expasy.org/protparam/>) was used to examine feature of physicochemical properties for instance, instability index, molecular weight, atomic composition,

theoretical pI, amino acid composition, Negative and Positive residues and grand average of hydropathicity (GRAVY) (Gasteiger et al. 2005; ProtParam 2017).

Membrane Topology prediction

We predicted Membrane topology and TM-helix position in such a particular cell of NSP4 protein by using TOPCON and SOSUI server and validate result with the help of signalP-4.0 server.

Secondary, Tertiary structure and model evaluation Predictions

Secondary structure prediction was implemented by SOPMA server which focuses on the analysis of maximum variances within each amino acids of alpha helix, beta sheet, and turns (Geourjon et al.1995). The sequence of NSP4 protein was submitted to SWISS-MODEL server for prediction of homology modelling. Server simultaneously performed BLASTp against PDB structure in order to find out best template which was assessed from target-template alignment topographies. After that, model with highest quality was recommended for model building (Arnold et al. 2006). Primary structure was employed to verify errors throughout 3D structure Structure was then analyzed and incorporated by using distinct types of programs and conformation servers such as ERRAT and verify 3D. RAMPAGE server has been used to generate Ramachandran plot and verify result by Procheck server (Dym et al. 2012). In this stage we were enabled to identify that residues of protein structure are locating in favored region, allowed and outlier region. We have done all visualization of current result by using USCF chimera 4.1 software (Rodríguez-Guerra et al. 2018).

Retrieval of Antiviral Phytochemical Compounds

Literature survey was performed to search phytochemical reported compounds against SARS-CoV-2. 3D structure of phytochemical compounds were obtained from PubChem database in sdf format (Kim et al. 2019). We performed optimization of all ligand structures with the help of Avogadro software and used in Molecular Operating Environment (MoE) ligand database for docking process.

Molecular docking

The MoE site finder tool and COACH server were used to identify reported binding pocket of NSP4 protein, and generating specific docking sites (Wu et al. 2018). MoE software was used for Docking of ligand database within defined docking sites of protein. All phytochemical compounds were classified on the basis of S-score. We used certain compounds for interaction study, based on highest docked score and active site binding to protein.

Ligand receptor interaction analysis

For better understanding of interactions, top ranked complexes were added to LigX tool of MoE, where it

generates 2D plots of receptor and ligand interaction analysis. This plot showed different types of bonding (eg, hydrogen bonding) and key interactions (electrostatic, and Van der Waals) which played a major role in the binding affinity of drug candidate with the active site of NSp4 protein. 3D complex structures of NSP4 protein with inhibitors were prepared through MOE software (Sapundzhi and Dzimbava 2018) and PyMOL.

ADME Toxicity/Drug Scan from AdmetSar Server

The drug likeness photochemical compounds were obtained based on Lipinski's rule of five, quality estimation of absorption, distribution, metabolism and excretion. Toxicity analysis of certain hits was also predicted virtually by using AdmetSar server (Cheng *et al.* 2012). In addition, AMES was also used to analyze the toxicity and carcinogenic properties of selected inhibitors.

RESULTS

Physiochemical properties of NSP4 protein

We submitted amino acid sequence of target protein to ExpAsy's ProtParam Server for calculating physiochemical properties. This server also predicts protein stability and steadiness. We investigated that molecular weight of NSP4 is 56183.98 kDa and consists of 500 amino acid residues forming a linear primary structure. An isoelectric point (PI) of protein is found 7.61 which facilitates positive charge on protein structure. Negative GRAVY index was 3.43 that demonstrates that protein was hydrophobic and soluble in nature. Most abundant residues were also detected as Valine (46), Leucine (49) and Glycine (41) tracked by Serine (38) and Alanine (36). The tryptophan (6) residues have found rarely in its structure. The protein sequence consists of 37 negative and positive charged residues (Aspartic acid, Glutamic) and (Arginine, lysine). Molecular formula of protein is $C_{2592}H_{3925}N_{631}O_{716}S_{25}$ while total number of atoms in protein is 7889.

Membrane topology of NSP4 protein

The prediction of subcellular localization of protein through computational studies that exists within cell, envisaging position of unidentified protein may provide indication of cellular functions and this evidence can be used for understanding the mechanism of disease and drug designing. The subcellular position of SARS-CoV-2 NSP4 protein was evaluated which describes that it is membranous protein having trans-membrane (TM) helices. The exact positions of these helices are predicted by TOPCON server originated from residues number TM1: 210-230, TM2: 242-262, TM3: 264-284, TM4: 286-306 and TM5: 308-328 as shown in Fig 1 (Tsirigos *et al.* 2015).

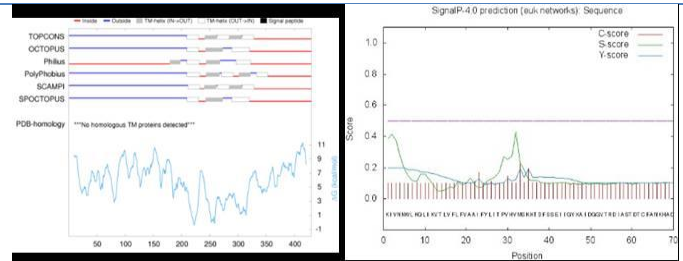


Figure1: (a)TOPCONS and (b) Signalp4 showed that NSP4 is present within the cell membrane.

Secondary and Tertiary structure NSP4 protein

Protein function is directly dependent on 3D structure recognized active site residues, and facilitates drug designing. The computational technique for structure prediction is easy then X-ray crystallography and NMR (Kopp & Schwede, 2004; Jaroszewski, 2009). The result of secondary structure indicates that random coils were present (28.20%) in NSP4 protein structure, which followed through extended strand (20.60%) while alpha helix was highly abundant (45.60%) and beta sheet as 5.60%(Fig.2).3D structure of NSP4 protein was predicted by employing SWISS MODEL which recognized best appropriated template 3vcv having sequence similarity of 61.36%, that was a virtuous score for building Model. 3D structure was analyzed through Discovery Studio and shown in Fig.3. Later on structure prediction properties of model was primarily checked by ERRAT that outlined statistics of non-bonded interaction within various categories of atoms and focused on atomic characteristic connection. Overall quality factor efficiency was 84.507 which is good for modeling (Colovos & Yeates, 1993). Model was verified by using PROSAweb server that described information about energy minimization and Z score. Z-score of NSP4 protein was found to be -4.34, that described model is virtuous, presented in Fig.4.

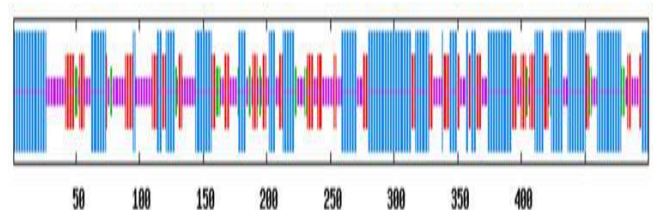


Figure 2: Graphical representation NSP4 secondary structure; Blue: shows alpha helix; Red; shows beta sheets; Orange: shows random coils

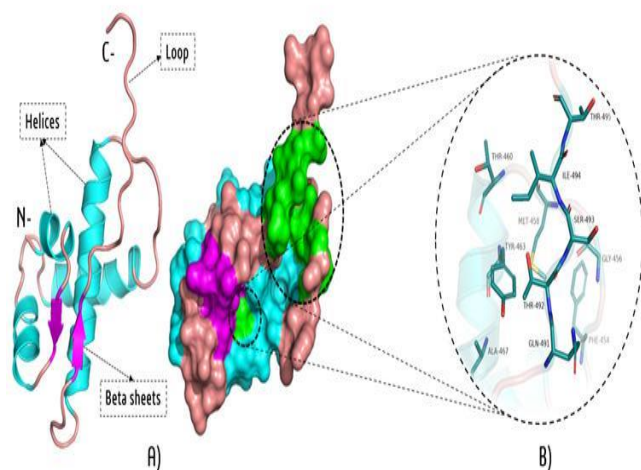


Figure 3: A) SARS-CoV-2 NSP4 predicted 3D structure and surface model; Purple: beta sheets structure; Deep salmon: loops structure; Cyan: predicted exposed helices region in NSP4 (b) Predicted active sites residues at alpha helix and loop regions showed in green color.

RAMANHANDRAN PLOT QUALITY ASSESMENT

Stereo chemical quality of NSP4 model was observed by means of Ramachandran plots through the Procheck server and validated by using RAMPAGE, residues of protein structure were confirmed and lie in different regions; favoured region (94.3%), allowed region (4.6%) and outlier region (1.1%). Our results demonstrated that predicted model shows a better-quality factor (Fig.4).

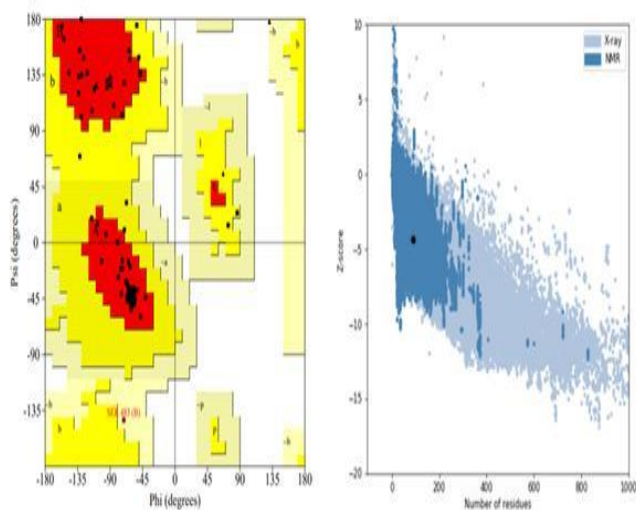


Figure 4: Ramachandran plot and Z-score analysis

Database Screening and Molecular Docking

We performed docking on antiviral phytochemical compounds against SARS-CoV-2 NSP4 protein model

and listed them on the basis of stringent screening which consists of four factor, maximum binding pockets presence with minimum Gibbs Free energy, hydrogen bonding, and other interactions were collectively predicted and described with an S-score function. MOE site finder tool and Coach Server predicted the active site residues of the NSP4 protein. Sitefinder predicted binding pocket containing the catalytic residues triad. Tyr448, Tyr451, Lys452, Tyr453, Phe454, Ser455, Gly456, Ala457, Met458, Asp459, Thr460, Tyr463, Ala466, Ala467, Cys469, His470, Pro490, Gln491, Thr492, Ser493, Ile494 and Thr495 were selected through site finder tool of MOE while Tyr463, Ala467 and Ala474 was the predicted sites residues from COACH server. Total 63 compounds were docked from which top ranked compounds were selected. LIG1(CID_7312251), LIG2(CID_5467200), LIG3(CID_10389806), LIG4(CID_5280343), LIG5(CID_3085830), LIG6(CID_10071695) and LIG7(CID_3080597) (Qamar *et al.* 2017) were found attached with high binding energy in the active site of NSP4 protein (Table 2). The residues of protein structure were represented in circles and colors characterized their types. Protein residues were seeming in distinct types of circle according to interaction studies and their color categorized their types. Hydrophobic residues were shown in green circle and deep purple represent polar charge residues. Acidic residues have been exhibited in red edge and basic residues with blue border while solvent exposure as a halo disc around residues in bluish color. The arrow of hydrogen bonds exhibited with dotted lines showing direction of bonds. Dotted lines arrow specified positions of residues in protein. Green represents side chain residues, yellow for solvent ion and blue for backbone residue (Yoshimoto *et al.* 2020).

Binding Interactions

SARS-COV-2 NSP4 have two lobes N terminal and C terminal in their structure. The reported inhibitor LIG1 was docked to NSP4 and exhibit -11.8711 Kcal/Mol binding energy that is shown in table (Table 2). Hydrogen bonds were located to side chain of arene-H with Tyr463 and backbone of Thr460, although Met458 other residues that associated closely were Ile494, Gln491, Thr492, Thr495, Ser493, Asp459, Gly456 and Ala457 (Fig.5A). The cut-off maximum distance of the interacting residues is 4.5 angstroms. LIG1 was followed by the LIG2, LIG3 and LIG4 with binding scores of -15.7308 , -15.3199 and -15.1762 kcal/mol respectively (Table 2).

Binding score of these inhibitors was higher than other compounds. Interaction pattern of LIG2 confirmed that it is facilitating hydrogen bonds with back-bone donor and side-chain donor of hydrophobic and polar residues Met454, Phe454 and Ser493 with $-OH$ group, while arene-arene and arene-H stacking interactions were formed with His470 and Gln491 with benzene ring. Apart of H-bonds, along with hydrophobic/vdW interactions were also recognized among the active site residues of protein.

Significant vdW/hydrophobic interactions with inhibitors were made by Gly456, Ser455, Tyr463, Tyr451, Thr460, Tyr448, Ala457 and Pro490 (Fig.5B). However, residues belonging to activation segment with LIG3 were catalytic polar residues. Thr492, Thr460 and Gln491 forms h-bonds/vdW as side-chain acceptor /back-bone donor with –OH groups and Carbonyl groups while Tyr463 formed arene-arene/vdW Hydrophobic residue. Met458 exposed h-bond/vdW as backbone acceptor/donor with –OH group. Strong and week hydrophobic/vdW interactions were found in residues (Leu417, Ala457, Thr495, Ile494 and Ser493) illustrated in Fig.5C. LIG4 exposed higher docking score owing to tendency of hydrogen bonds with polar residues bind as backbone acceptor/donor. The catalytic residues Gly456, Phe454 and Ser493 indicated h-bonds with Carbonyl group and –OH group.

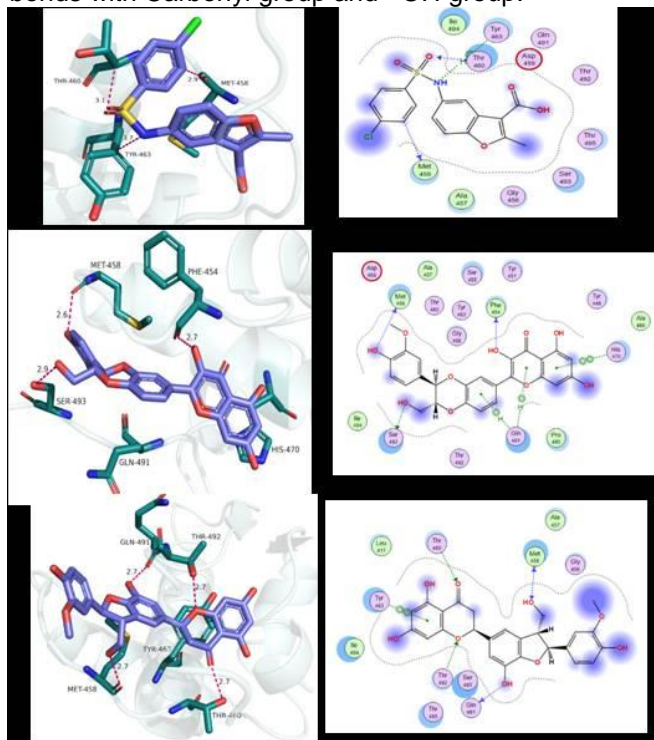


Figure 5: 2D and 3D interaction analysis of LigX tool of MoE and PyMOL which highlight the distances and H-bonds interaction between NSP4 active site residues and inhibitors. (A) Docking pattern of LIG1 showed the maximum distance 3.9 Å. (B) Docking pattern of LIG2 indicated the extreme distance 2.9 Å. (C) Docking Pattern of LIG3 facilitated with the equal Gln491 Ser493 and Ala457 participating in non-

Other residues which mediate the spatial interactions with LIG4 was Pro490, Gln491, Met458, Tyr463, Tyr451 and Thr492 are displayed in Fig.6D. The S-score of LIG5 -14.4894 was observed with strong h-bonds to the active site residues. The catalytic polar and hydrophobic His470, Gly456, Phe454, Thr496 and Lys452 (residues of activation segments) were existing near the vicinity of –OH groups as backbone acceptor/donor as well as side

chain donor, while Ile494 showed arene-H with benzene ring of inhibitor.

Instead of these pivotal stacking interactions between LIG5 and active sites residues involves Tyr451, Tyr448, Pro490, Thr492, Tyr463, Ser493 and Met458 forming hydrophobic/vdW as explained in Table 2 and Fig. 6E. The S-score of LIG6 was -14.1884 (Table 2) observed the Carbon of benzene ring of inhibitor exhibits hydrogen bond as side chain acceptor with polar residue Thr492. The other residues showed interactions around the LIG6 were Ile494, Tyr463, Gln491, Ser493, Thr460, Met458, Gly456 and Ser455 (Fig.6f) while in (Fig.6g)

LIG7 specified H-bonding with Carbonyl group induces strong side-chain donor with polar residue Thr495 and hydrophobic residue Met458 exhibits h-bond as backbone donor having minimum S-score energy -9.4838 as detailed in Table 2. Ile494, Ala457, Thr460, Ser493 and Tyr463 are found as hydrophobic/vdW interactions around LIG7.

covalent bonding.

Hydrophobic interactions Gln491 Ser493 and Ala457 participating in non-covalent bonding. Hydrophobic interactions Gln491 Ser493 and Ala457 participating in non-covalent bonding. Hydrophobic interactions which are necessary structurally and functionally to SARS-COV-2 NSP4 protein. However out of all inhibitors LIG2, LIG3, LIG4 were placed at topmost because it exhibited highest binding energy and more interaction bonding propensities.

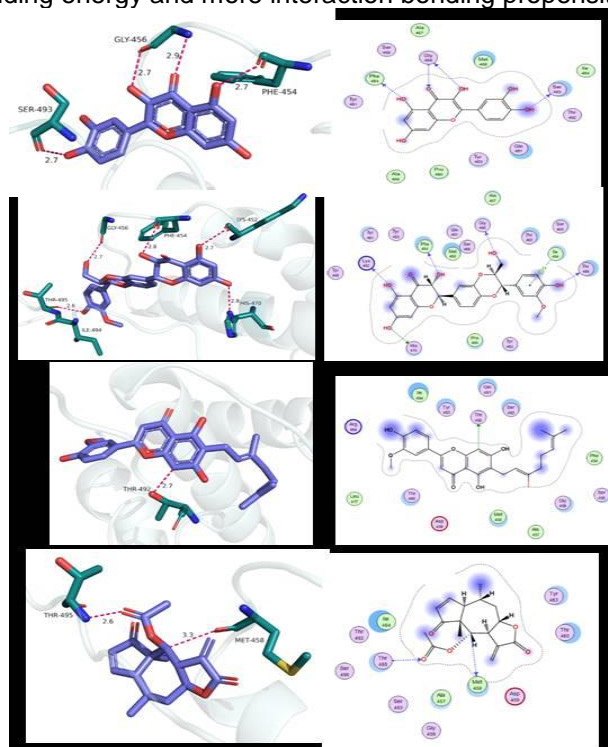


Figure 6: (D) Docking pattern of LIG4 exposed the top distance 2.9 Å. (E) Docking pattern of LIG5 explored

the supreme distance 2.8 Å. (F) Docking pattern of LIG6 revealed the distance 2.7 Å. (G) Docking pattern of LIG7 showed the distance limit 3.3Å

ADMET/Drug Scan results

ADMETsar sever were used for prediction of drug likeness and ADMET properties of compounds. Entire photochemical compounds are non-toxic, non-

carcinogenic passes Lipinski rule of five with 0 violations. The numbers of conformational changes of molecules were described by the number of rotatable bonds and also for the binding ability to receptor for use as drug candidate. All inhibitors passed ADMETsar threshold of drug ability as shown in table (Table 1 and 3).

Table 1: Molecular properties and drug likeliness of phytochemicals

Photochemical Name	LIG. No	Molecular formula	Molecular weight	Log p	H- bond donor	H- bond acceptor	Rotatable bond
5-{{(4-chlorophenyl) sulfonyl}amino}-2-methyl-1-benzofuran-3-carboxylic acid	LIG1	C16H12ClNO5S	365.8g/mol	3.89	2	4	4
2,3-Dehyrosilybin	LIG2	C25H20O10	480.4g/mol	3.16	5	10	4
Silyhermin	LIG3	C25H22O9	446.4g/mol	3.34	5	9	4
Quercetin	LIG4	C15H10O7	302.24g/mol	1.99	5	7	1
Isosilybin	LIG5	C25H22O10	482.4g/mol	2.36	5	10	4
Cannflavin A	LIG6	C26H28O6	436.50g/mol	5.0	3	6	7
Bigelovin	LIG7	C17H20O5	304.34g/mol	1.82	0	5	1

Table 2: Summary of top ranked phytochemicals screened against NSP4. Active sites residues with their respective docking score, interacting residues and residues contact.

Photochemical Name	LIG. No	S-score	Interaction f Residues with inhibitors through H-Bonding	All residues contact around the Inhibitors
5-{{(4-Chlorophenyl) sulfonyl}amino}-2-methyl-1-benzofuran-3-carboxylic acid	LIG1	-11.8711	Tyr463, Met458, Thr460	Ile495, Thr495, Ser493, Ala457, Thr492, Gln491, Asp459, Gly456
2,3-Dehyrosilybin	LIG2	-15.7308	Met458, Ser493, Phe454, Gln491, His470	Ile494, Tyr463, Tyr451, Tyr448, Ser455, Gly456, Ala457, Ala466, Thr492, Pro490, Thr460, Asp459
Silyhermin	LIG3	-15.3199	Met458, Thr492, Ser493, Thr460, Gln491	Ile494, Tyr463, Gly456, Ala457, Thr495, Leu417, Asp459, Arg464
Quercetin	LIG4	-15.1762	Gly456, Ser493, Phe454	Met458, Tyr463, Gln491, Tyr451, Ser456, Ala457, Pro490, Ile494, Thr492, Ala466
Isosilybin	LIG5	-14.4894	Met458, Gly456, Thr495, Ile494, His470, Lys452, Gln491,	Tyr451, Tyr463, Tyr453, Tyr448, Ser455, Ser493, Thr492, Thr460, Ala457, Ala466, Phe454, Pro490, Gln491, Asp459
Cannflavin A	LIG6	-14.1884	Thr492	Tyr463, Ile494, Met458, Ser493, Gln491, Gly456, Ser455, Thr460, Arg464, Phe454, Ala457, Leu417, Asp459
Bigelovin	LIG7	-9.4838	Met458, Thr495	Tyr463, Ile494, Thr460, Thr492, Ala457, Ser493, Ser496, Asp459, Gly456

Table 3: ADMET Profiling Enlisting Absorption, Metabolism and Toxicity related drug like parameters of all inhibitors

Model	5-[[[4-Chlorophenyl) Sulfonyl]Amino]-2-Methyl-1-Benzofuran-3-Carboxylic Acid	2,3-Dehydrosilybin	Silyhermin	Quercetin	Isosilybin	Cannflavin A	Bigelovin
Absorption							
Blood-Brain Barrier	BBB+	BBB-	BBB-	BBB-	BBB-	BBB+	BBB+
Human Intestinal absorption	HIA+++	HIA+	HIA+	HIA+	HIA+	HIA+	HIA+
Caco-2 permeability	Caco2+	Caco2-	Caco2-	Caco2-	Caco2-	Caco2-	Caco2+
p-glycoprotein substrate	Non substrate	Non substrate	Non substrate	Non substrate	Non substrate	Non substrate	Non substrate
p-glycoprotein inhibitor	Non inhibitor	Inhibitor	Inhibitor	Non inhibitor	Inhibitor	Inhibitor	Non inhibitor
Metabolism							
CYP4502C9 substrate	Non substrate	Non substrate	Non substrate	Non substrate	Non substrate	Non substrate	Non substrate
CYP4502D6 substrate	Non substrate	Non substrate	Non substrate	Non substrate	Non substrate	Non substrate	Non substrate
CYP450 3A4 Substrate	Non substrate	Substrate	Substrate	Substrate	Substrate	Substrate	Substrate
CYP450 1A2 Inhibitor	Inhibitor	Inhibitor	Non inhibitor	Inhibitor	Non inhibitor	Inhibitor	Non inhibitor
CYP450 2C9 inhibitor	Inhibitor	Inhibitor	Inhibitor	Inhibitor	Inhibitor	Inhibitor	Non inhibitor
CYP450 2D6 inhibitor	Non inhibitor	Non inhibitor	Non inhibitor	Non inhibitor	Non inhibitor	Non inhibitor	Non inhibitor
CYP450 2C19	Non inhibitor	Non inhibitor	Inhibitor	Non inhibitor	Non inhibitor	Inhibitor	Non inhibitor
CYP450 3A4 inhibitor	Non inhibitor	Inhibitor	Inhibitor	Inhibitor	Inhibitor	Non inhibitor	Non inhibitor
Toxicity							
AMES Toxicity	Non-Ames toxic	Non-Ames toxic	Non-Ames toxic	Non-Ames toxic	Non-Ames toxic	Non-Ames toxic	Non-Ames toxic
Carcinogens	Non carcinogens	Non carcinogens	Non carcinogens	Non carcinogens	Non carcinogens	Non carcinogens	Non carcinogens

DISCUSSION

Corona virus has become a pandemic since it is spreading and affecting the people around the world. The correlative factor SARS-CoV-2 has demonstrated to be dangerous and caused severe public health issues globally. While spreading of SARS in 2003 and MERS-CoV in 2012 provoked the comprehensive work there were no medicine for treatment of Zoonotic Corona virus. SARS virus is appeared 17 years ago and SARS-CoV-2 is seemed in corona virus that continue to present a serious threat to global public health. The recent upsurge is to attempt and finding of critical antiviral preventative therapeutic drug because there is no FDA approval drug in the market as yet. The designing of vaccine against SARS-CoV-2 disease have major challenge to world, researcher still working on developing of vaccines but it's too late that affect very much peoples (Amanat and Krammer 2020). The essential residues of amino acids are indeed to provoked membrane reconfiguration of NSP4 protein by interaction with NSP3.

In our current study we focused on homology modelling of NSP4 protein and molecular docking with the help of bioinformatic tool and server, and predicted structure was selected for docking against 63 antiviral phytochemical compounds. These compounds were retrieved from PubChem data base and exhibits high binding scores against targeted protein. We selected only 7 compounds on the basis of their best energy and h-bonding and interaction from high throughput virtual screening. These seven phytochemical compounds LIG1, LIG2, LIG3, LIG4, LIG5, LIG6 and LIG7 have possible interaction and important hydrophobic contact with active site residues of NSP4 protein. These compounds have fulfilled "Lipinski's Rule of five", (Brito 2011) (Table 1). Mostly drug molecules omit through drug development process due to its poor pharmacokinetic properties and toxicity (Mota *et al.* 2018). ADMET profiling of compounds reveals that there were no side effects on absorption. Compounds concentrations levels in brain is determined by the blood brain barrier (BBB). One of key aspects to be optimized compounds in drug development and its distribution of drug molecules via blood brain barrier. BBB is generated within the capillaries of endothelial cell by the existence of maximum strength of close junction that prohibits brain uptake (Stokum *et al.* 2016; Li *et al.* 2019). Oral bioavailability is also used as an important factor in assessing drug likeness active compounds as therapeutic agents (Bickerton *et al.* 2012). In fact, physiological, physicochemical, and also some others biopharmaceutical factor may greatly affect oral bioavailability (Hurst *et al.* 2007). In the case of active drug molecule is passing out through central nervous system (CNS), increasing prevalence of the blood brain is required whereas non-CNS low penetration is desirable to remove CNS consequences (Araujo *et al.* 2012). ADMET attributes

possible and various model, for instance p-glycoprotein substrate, human intestinal absorption, BBB penetration, and CaCO₂ permeability demonstrated positive results that clearly affirm potential of compounds to serve as drug candidates. HIA has been one of major stages throughout the transportation of drug molecules to their targets, these compounds LIG2, LIG3, LIG4 and LIG5 having negative results towards Blood brain barrier while LIG1, LIG6 and LIG7 demonstrate positive results. CaCO₂ permeability showed negative results except LIG1 and LIG7. HIA exhibits positive results of all inhibitors, a group of isoenzymes such as Cytochrome P450 (CYP) engaged in the metabolisms of drugs, bile acids, and steroids. Human genome encodes fifty-seven CYP in which fifteen were concerned in Xenobiotic chemicals as well as others were involved in metabolism of drugs (Saravanakumar *et al.* 2019). Around 75% metabolism of drug molecules relies interaction to CYP enzyme. It is found that all inhibitors were non-toxic, and isolated in *Silybum marianum*, *W. somnifera*, *Inula helianthus-aquatic* and *Cannabis sativa L.* In previous research phenolic compounds were obtained from *Silybum marianum* and used as antiviral against herpessimplex virus, type 2 (HSV-2), compounds were also used in docking study that exhibit strong docking score and interaction to estrogen receptor (Zava *et al.* 1998; Zierau *et al.* 2002). Extracts of *Inula helianthus-aquatica* leaves have antidiabetic activity (Seca *et al.* 2015), anti-inflammatory activity, antiviral and antimicrobial activity (Zeng *et al.* 2009). Extracts of *Cannabis sativa L* have potential antiviral activity (Mukhtar *et al.* 2008; Girgih *et al.* 2011) and antioxidant activity while the extracts of *W. somnifera* have antiviral activity (Kambizi *et al.* 2007). We may therefore infer that selected inhibitors may be used as a novel and effective drug candidate against SARS-COV-2 NSP4 protein.

CONCLUSION

The current research considers the selective inhibition of the NSP4 Protein, which is active in corona virus membrane replication. Similar inhibitors are identified for NSP4 protein focusing on multitarget drug approach. Homology modeling and Molecular docking has been used to find possible inhibitors for NSP4 proteins and to explore the important residues involves in inhibitor binding to the protein active site.

Seven NSP4 inhibitors have been described out of 200 antiviral phytochemical compounds, all of which act by competing with the active site. The formation of hydrogen bonds within the active region of the protein is being used as the primary criterion for evaluating strong inhibitor binding. Apart from hydrogen bonds, hydrophobic as well as van der waal interactions are the critical partners in this system.

Because of their high binding energy and interaction pattern, LIG2, LIG3, LIG4, LIG5, and LIG6 proved to be the strongest binders for everything. This study will

expedite the development of multi-target medicines against NSP4 proteins, that could be used to develop novel therapies for a variety of diseases.

CONFLICT OF INTEREST

The authors declared that present study was performed in absence of any conflict of interest.

ACKNOWLEDGEMENT

The author(s) received no financial support for the research, authorship, and/or publication of this article.

AUTHOR CONTRIBUTIONS

Conceived and designed the proposal: Aamir Saeed and Huma Naseem; Analyzed and Performed *In-silico* data: Aamir Saeed and Huma Naseem; Manuscript written by Huma Naseem, Aamir Saeed, Basharat Ahmad and Nighat Shafi; Reviewed by: All authors read and approved the final manuscript.

Copyrights: © 2022@ author (s).

This is an open access article distributed under the terms of the [Creative Commons Attribution License \(CC BY 4.0\)](https://creativecommons.org/licenses/by/4.0/), which permits unrestricted use, distribution, and reproduction in any medium, provided the original author(s) and source are credited and that the original publication in this journal is cited, in accordance with accepted academic practice. No use, distribution or reproduction is permitted which does not comply with these terms.

REFERENCES

- Abraham MH (2004). The factors that influence permeation across the blood-brain barrier. *Eur. J. Med. Chem.*, 39: 235-240.
- Amanat, F., & Krammer, F. (2020). SARS-CoV-2 vaccines: status report. *Immunity*.
- Araujo F, Nogueira R, Araujo MS, Perdigao A, Cavalcanti L, Brilhante R, Rocha M, Vilar DF, Holanda SS, Braga Dde M and Sidrim J (2012). Dengue in patients with central nervous system manifestations, Brazil. *Emerg Infect Dis.*, 18: 677-679.
- Arnold K., L. Bordoli, J. Kopp, T. Schwede (2006). The SWISS-MODEL Workspace: A Web-based Environment for Protein Structure Homology Modelling, *Bioinformatics*, 22(2), 195-201.
- Astuti, I. (2020). Severe Acute Respiratory Syndrome Coronavirus 2 (SARS-CoV-2): An overview of viral structure and host response. *Diabetes & Metabolic Syndrome: Clinical Research & Reviews*.
- Balunas, M. J., & Kinghorn, A. D. (2005). Drug discovery from medicinal plants. *Life sciences*, 78(5), 431-441.
- Benkert P., M. Biasini, T. Schwede (2011). Toward the Estimation of the Absolute Quality of Individual Protein Structure Models, *Bioinformatics*, 27(3), 343-350.
- Bickerton, G. R., Paolini, G. V., Besnard, J., Muresan, S.,

- & Hopkins, A. L. (2012). Quantifying the chemical beauty of drugs. *Nature chemistry*, 4(2), 90-98.
- Boopathi, S., Poma, A. B., & Kolandaivel, P. (2020). Novel 2019 coronavirus structure, mechanism of action, antiviral drug promises and rule out against its treatment. *Journal of Biomolecular Structure and Dynamics*, 1-10.
- Brito, M. A. D. (2011). Pharmacokinetic study with computational tools in the medicinal chemistry course. *Brazilian Journal of Pharmaceutical Sciences*, 47(4), 797-805.
- Cardile, A. P., & Mbuy, G. K. (2013). Anti-herpes virus activity of silibinin, the primary active component of *Silybum marianum*. *Journal of Herbal Medicine*, 3(4), 132-136.
- Cheng, F., Li, W., Zhou, Y., Shen, J., Wu, Z., Liu, G., ... & Tang, Y. (2012). admetSAR: a comprehensive source and free tool for assessment of chemical ADMET properties.
- Cheng, F., Li, W., Zhou, Y., Shen, J., Wu, Z., Liu, G., ... & Tang, Y. (2012). admetSAR: a comprehensive source and free tool for assessment of chemical ADMET properties.
- Cotten, M., Watson, S. J., Kellam, P., Al-Rabeeah, A. A., Makhdoom, H. Q., Assiri, A., ... & Al Hajjar, S. (2013). Transmission and evolution of the Middle East respiratory syndrome coronavirus in Saudi Arabia: a descriptive genomic study. *The Lancet*, 382(9909), 1993-2002.
- Dym, O., Eisenberg, D., & Yeates, T. O. (2012). PROCHECK.
- Gasteiger E., C. Hoogland, A. Gattiker, S. Duvaud, M. R. Wilkins, R. D. Appel, A. Bairoch (2005). Protein Identification and Analysis Tools on the ExPASy Server, In: *The Proteomics Protocols Handbook*, Walker J. M. (Ed.), Humana Press, 571-607.
- Geourjon C., G. Deléage (1995). SOPMA: Significant Improvements in Protein Secondary Structure Prediction by Consensus Prediction from Multiple Alignments, *Computer Applications in Biosciences*, 11(6), 681-684
- Girgih, A. T., Udenigwe, C. C., & Aluko, R. E. (2011). In vitro antioxidant properties of hemp seed (*Cannabis sativa* L.) protein hydrolysate fractions. *Journal of the American Oil Chemists' Society*, 88(3), 381-389.
- Goodwin, J. T., & Clark, D. E. (2005). In silico predictions of blood-brain barrier penetration: considerations to "keep in mind". *Journal of Pharmacology and Experimental Therapeutics*, 315(2), 477-483.
- Guo, Y. R., Cao, Q. D., Hong, Z. S., Tan, Y. Y., Chen, S. D., Jin, H. J., ... & Yan, Y. (2020). The origin, transmission and clinical therapies on coronavirus disease 2019 (COVID-19) outbreak—an update on the status. *Military Medical Research*, 7(1), 1-10.
- Gupta, A., Siew, M., & Subramaniam, B. B. Thromboembolism in Covid 19.
- Gupta, M. K., Vemula, S., Donde, R., Gouda, G., Behera,

- L., & Vadde, R. (2020). In-silico approaches to detect inhibitors of the human severe acute respiratory syndrome coronavirus envelope protein ion channel. *Journal of Biomolecular Structure and Dynamics*, 1-11.
- Huang, C., Wang, Y., Li, X., Ren, L., Zhao, J., Hu, Y., ... & Cheng, Z. (2020). Clinical features of patients infected with 2019 novel coronavirus in Wuhan, China. *The lancet*, 395(10223), 497-506.
- Hurst, S., Loi, C. M., Brodfuehrer, J., & El-Kattan, A. (2007). Impact of physiological, physicochemical and biopharmaceutical factors in absorption and metabolism mechanisms on the drug oral bioavailability of rats and humans. *Expert opinion on drug metabolism & toxicology*, 3(4), 469-489.
- Kambizi, L. G. B. M., Goosen, B. M., Taylor, M. B., & Afolayan, A. J. (2007). Anti-viral effects of aqueous extracts of *Aloe ferox* and *Withania somnifera* on herpes simplex virus type 1 in cell culture. *South African Journal of Science*, 103(9-10), 359-360.
- Kanjanahaluethai, A., Chen, Z., Jukneliene, D., & Baker, S. C. (2007). Membrane topology of murine coronavirus replicase nonstructural protein 3. *Virology*, 361(2), 391-401.
- Kim, S., Chen, J., Cheng, T., Gindulyte, A., He, J., He, S., ... & Bolton, E. E. (2019). PubChem 2019 update: improved access to chemical data. *Nucleic acids research*, 47(D1), D1102-D1109.
- Li, Q., Guan, X., Wu, P., Wang, X., Zhou, L., Tong, Y., ... & Xing, X. (2020). Early transmission dynamics in Wuhan, China, of novel coronavirus-infected pneumonia. *New England Journal of Medicine*.
- Li, Y., Meng, Q., Yang, M., Liu, D., Hou, X., Tang, L., ... & Bi, H. (2019). Current trends in drug metabolism and pharmacokinetics. *Acta Pharmaceutica Sinica B*, 9(6), 1113-1144.
- Lipinski C.A., Lombardo F. et al. Experimental and computational approaches to estimate solubility and permeability in drug discovery and development settings. *Adv. Drug Deliv. Rev.* 2012, 64, 4–17
- López-Vallejo F., Caulfield, T., et al Integrating virtual screening and combinatorial chemistry for accelerated drug discovery. *Comb. Chem. High Throughput Screen.* 2011, 14, 475–487.
- Meng, X.Y.; Zhang, H.X.; Mezei, M.; Cui, M. Molecular docking: A powerful approach for structure-based drug discovery. *Curr. Comput. Aided Drug Des.* 2011, 7, 146–157
- Mota, C., Coelho, C., Leimkühler, S., Garattini, E., Terao, M., Santos-Silva, T., & Romão, M. J. (2018). Critical overview on the structure and metabolism of human aldehyde oxidase and its role in pharmacokinetics. *Coordination Chemistry Reviews*, 368, 35-59.
- Mukhtar, M., Arshad, M., Ahmad, M., Pomerantz, R. J., Wigdahl, B., & Parveen, Z. (2008). Antiviral potentials of medicinal plants. *Virus research*, 131(2), 111-120.
- Oany A. R., S. A. I. Ahmad, M. A. A. Siddiquey, M. U. Hossain, A. Ferdoushi (2014). Computational Structure Analysis and Function Prediction of an Uncharacterized Protein (I6U7D0) of *Pyrococcus furiosus* COM1, *Austin J Comput Biol Bioinform*, 1(2):5.
- Oany A. R., T. P. Jyoti, S. A. Ahmad (2014). An in silico Approach for Characterization of an Aminoglycoside Antibiotic-resistant Methyltransferase Protein from *Pyrococcus furiosus* (DSM 3638), *Bioinformatics and Biology Insights*, 8, 65-72.
- Oostra, M., Hagemeyer, M. C., Van Gent, M., Bekker, C. P., Te Lintelo, E. G., Rottier, P. J., & De Haan, C. A. (2008). Topology and membrane anchoring of the coronavirus replication complex: not all hydrophobic domains of nsp3 and nsp6 are membrane spanning. *Journal of virology*, 82(24), 12392-12405.
- Oostra, M., Te Lintelo, E. G., Deijis, M., Verheije, M. H., Rottier, P. J. M., & De Haan, C. A. M. (2007). Localization and membrane topology of coronavirus nonstructural protein 4: involvement of the early secretory pathway in replication. *Journal of virology*, 81(22), 12323-12336.
- ProtParam, E. (2017). ExPASy-ProtParam tool. *SIB: Lausanne, Switzerland*.
- Qamar, M. T., Ashfaq, U. A., Tusleem, K., Mumtaz, A., Tariq, Q., Goheer, A., & Ahmed, B. (2017). In-silico identification and evaluation of plant flavonoids as dengue NS2B/NS3 protease inhibitors using molecular docking and simulation approach. *Pak. J. Pharm. Sci*, 30(6), 2119-2137.
- Rodríguez-Guerra Pedregal, J., & Maréchal, J. D. (2018). PyChimera: use UCSF Chimera modules in any Python 2.7 project. *Bioinformatics*, 34(10), 1784-1785.
- Sakai Y, Kawachi K, Terada Y, Omori H, Matsuura Y, Kamitani W (2017) Two-amino acids change in the nsp4 of SARS coronavirus abolishes viral replication. *Virology* 510:165–174
- Sakai, Y., Kawachi, K., Terada, Y., Omori, H., Matsuura, Y., & Kamitani, W. (2017). Two-amino acids change in the nsp4 of SARS coronavirus abolishes viral replication. *Virology*, 510, 165-174.
- Salgarello, M., Visconti, G., & Barone-Adesi, L. (2013). Interlocking circumareolar suture with undyed polyamide thread: a personal experience. *Aesthetic plastic surgery*, 37(5), 1061-1062.
- Sapundzhi, F. I., & Dzimbava, T. A. (2018). Computer modelling of the CB1 receptor by molecular operating environment. *Bulgarian Chemical Communications*, 50(Special Issue B), 15-19.
- Saravanakumar, A., Sadighi, A., Ryu, R., & Akhlaghi, F. (2019). Physicochemical properties, biotransformation, and transport pathways of established and newly approved medications: a systematic review of the top 200 most prescribed drugs vs. the FDA-approved drugs between 2005

- and 2016. *Clinical pharmacokinetics*, 58(10), 1281-1294.
- Seca, A. M., Pinto, D. C., & Silva, A. M. (2015). Metabolomic profile of the genus *Inula*. *Chemistry & biodiversity*, 12(6), 859-906.
- Stokum, J. A., Gerzanich, V., & Simard, J. M. (2016). Molecular pathophysiology of cerebral edema. *Journal of Cerebral Blood Flow & Metabolism*, 36(3), 513-538.
- Thomas VH, Bhattachar S, Hitchingham L, Zocharski P, Naath M and Surendran N (2006). The road map to oral bioavailability: An industrial perspective. *Expert Opin. Drug Metab. Toxicol.*, 2:591-608.
- Tsirigos, K. D., Peters, C., Shu, N., Käll, L., & Elofsson, A. (2015). The TOPCONS web server for consensus prediction of membrane protein topology and signal peptides. *Nucleic acids research*, 43(W1), W401-W407.
- Using Sequence Motifs for Enhanced Neural Network Prediction of Protein Distance Constraints. J. Gorodkin, O. Lund, C. A. Andersen, and S. Brunak In proceedings of the Seventh International Conference for Molecular Biology, eds. T. Lengauer, R. Schneider, P. Bork, D. Brutlag, J. Glasgow, H-W. Mewes, and R. Zimmer: 95-105, 1999.
- Walters, W. P. (2012). Going further than Lipinski's rule in drug design. *Expert opinion on drug discovery*, 7(2), 99-107.
- Wu, Q., Peng, Z., Zhang, Y., & Yang, J. (2018). COACH-D: improved protein–ligand binding sites prediction with refined ligand-binding poses through molecular docking. *Nucleic acids research*, 46(W1), W438-W442.
- Yoshimoto, F. K. (2020). The Proteins of Severe Acute Respiratory Syndrome Coronavirus-2 (SARS CoV-2 or n-COV19), the Cause of COVID-19. *The Protein Journal*, 1.
- Zava, D. T., Dollbaum, C. M., & Blen, M. (1998). Estrogen and progestin bioactivity of foods, herbs, and spices. *Proceedings of the Society for Experimental Biology and Medicine*, 217(3), 369-378.
- Zeng, G. Z., Tan, N. H., Ji, C. J., Fan, J. T., Huang, H. Q., Han, H. J., & Zhou, G. B. (2009). Apoptosis inducement of bigelovin from *Inula helianthus-aquatica* on human Leukemia U937 cells. *Phytotherapy Research: An International Journal Devoted to Pharmacological and Toxicological Evaluation of Natural Product Derivatives*, 23(6), 885-891
- Zhu N, Zhang D, Wang W, Li X, Yang B, Song J, Zhao X, Huang B, Shi W, Lu R et al: A Novel Coronavirus from Patients with Pneumonia in China, 2019. *N Engl J Med* 2020, 382(8):727-733.
- Zierau, O., Bodinet, C., Kolba, S., Wulf, M., & Vollmer, G. (2002). Antiestrogenic activities of *Cimicifuga racemosa* extracts. *The Journal of steroid biochemistry and molecular biology*, 80(1), 125-130.